

# Accounting for spray vaporization in turbulent combustion modeling

By J. Réveillon<sup>1</sup> AND L. Vervisch<sup>1</sup>

Three dimensional Direct Numerical Simulations (DNS) of droplet vaporization in the presence of turbulent micromixing have been performed. The transport equations for basic components of non-premixed turbulent combustion modeling, namely the mean of the mixture fraction and its fluctuations, are presented for the case of a dilute spray. The unclosed terms describing vaporization in the equation for the fluctuations of mixture fraction are analyzed via the DNS data, and a One Droplet Model (ODM) is proposed for those terms.

---

## 1. Introduction

Liquid fuel injection is one of the most common procedures in devices where non-premixed turbulent flames are utilized (e.g. diesel engines, aeronautical combustion chambers, and furnaces). Although much work has been devoted to gas-phase turbulent combustion modeling (Borghì 1988, Poinso *et al.* 1995, Bray 1996), relatively few studies have focused on the development of combustion models accounting for spray vaporization. Thus, when either Reynolds Averaged Navier Stokes Simulation (RANS) or Large Eddy Simulation (LES) are considered for the calculation of practical combustion chambers, turbulent combustion models accounting for spray vaporization are strongly needed.

Nonpremixed combustion is usually approached using conserved scalars where the mixture fraction,  $Z$ , and the magnitude of its gradient,  $|\nabla Z|$ , are used to parameterize the flame in analytical studies (Liñán 1974). In RANS or LES of non-premixed turbulent flames (Peters 1986, Pierce & Moin 1998),  $\tilde{Z}$ , the mean of the mixture fraction, together with  $\widetilde{Z''^2}$ , its level of fluctuation, are used in most combustion models. These quantities measure the extent of mixing between fuel and air, and along with the mixture fraction dissipation rate  $\overline{\rho\chi} = \overline{\rho D |\nabla Z''|^2}$  are used to estimate a micro-mixing time scale. When vaporization of fuel occurs,  $Z$  is not a conserved scalar due to local sources of fuel, resulting in additional unclosed terms appearing in the transport equations for  $\tilde{Z}$  and  $\widetilde{Z''^2}$ .

We have used DNS to simulate a dilute spray for the study of the vaporization terms found in the transport equation for  $\widetilde{Z''^2}$ . From the results, we discuss modeling of terms using the conditional mean value of the vaporization source of fuel, the conditioning quantity being the mixture fraction. Analytical results characterizing a dilute spray are utilized to derive an expression for this conditional mean value.

<sup>1</sup> LMFN, UMR CNRS 6614-CORIA, University and INSA of Rouen.

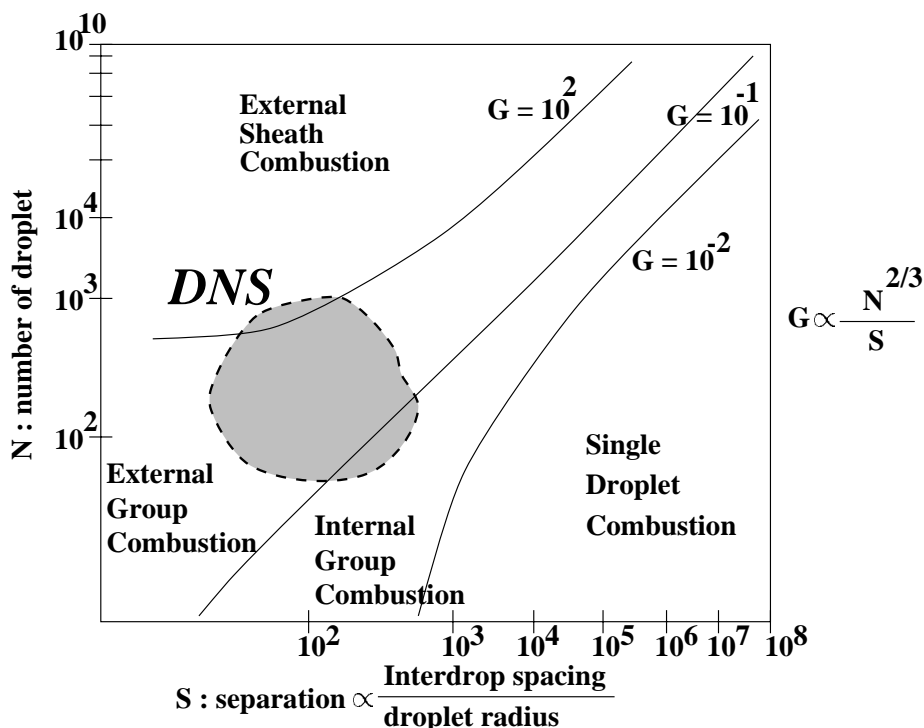


FIGURE 1. Classification of spray combustion regime. Group combustion diagram of Chiu *et al.* (1982).

The results are based on exact solutions obtained for a single droplet vaporizing in a given volume. Then, the accuracy of this One Droplet Model (ODM) is compared against the DNS data. These problems involving a dilute spray mimic situations that may be observed in aeronautical or rocket engines at a particular stage of the combustion process (Borghini 1996).

At the end of this report, the case of a flame attached to a droplet laden jet is also discussed as a challenging problem for DNS.

## 2. DNS of a turbulent spray

### 2.1 Introduction

Direct numerical simulation, in theory, allows for a model-free simulation; however, the resources required to perform the simulation of both the turbulent gas phase and the detailed motion of the liquid phase are too great. In our simulations, the flows around an individual drop and inside the drop are not fully resolved; instead available closures are introduced for the liquid phase along with its vaporization rate (Faeth 1983, Law 1982, Sirignano 1983). A Lagrangian description of the spray with two-way coupling (Faeth 1983) is employed. These simulations are restricted to droplets that are smaller than the Kolmogorov length scale. Therefore, in the group combustion diagram of Chiu *et al.* (1982) classifying different combustion regimes (Fig. 1), the present simulations are limited to problems observed in external combustion around clusters of droplets.

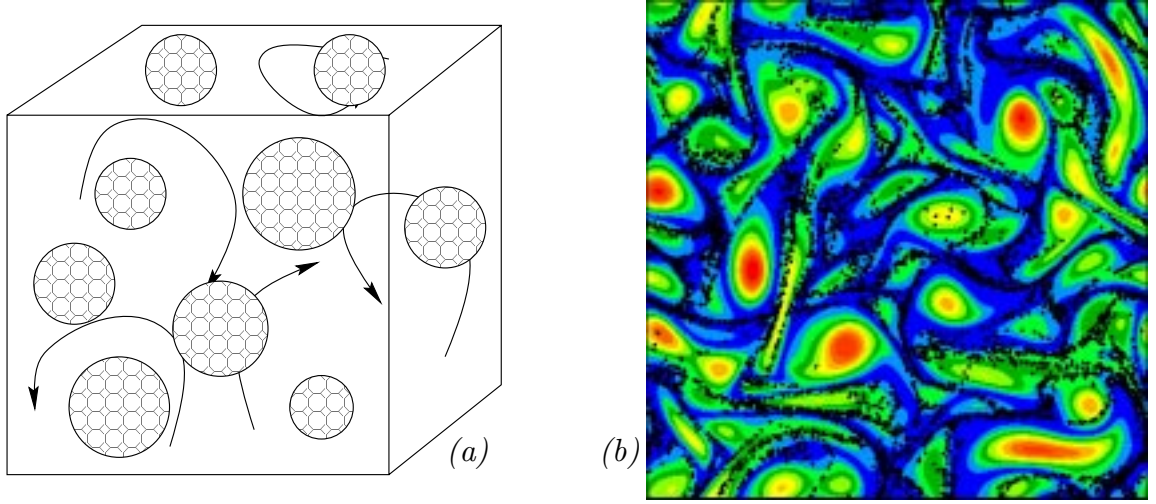


FIGURE 2. (a) Sketch of the initial repartition of the droplets. (b) 2D-snapshot of clusters dispersion after one eddy turn over time. Isolines: vorticity; dot: droplets.

### 2.2 Governing equations and numerics

A Lagrangian description is adopted for modeling the spray of fuel. The properties of the droplets are estimated by solving a system of three equations for each droplet: its position  $X^k$ , its diameter  $\Theta^k$ , and its velocity  $V^k$ . This system (Faeth 1983, Kuo 1986) may be written for each droplet as:

$$\begin{aligned} \frac{dX_i^k}{dt} &= V_i^k \quad , \\ \frac{d(\Theta^k)^3}{dt} &= -Aw_v^k \quad , \\ \frac{d(\Theta^k)^3 V_i^k}{dt} &= A(D_i^k - w_v^k V_i^k) \quad , \end{aligned}$$

with the mass evaporation rate and drag force given by:

$$\begin{aligned} w_v^k &= \pi \frac{\mu S_{hc}^k}{Re S_c} \ln(1 + B_Y^k) \Theta^k \quad , \\ D_i^k &= \frac{\pi}{8} \rho (\Theta^k)^2 C_D^k |U_i^k - V_i^k| (U_i^k - V_i^k) \quad , \end{aligned} \quad (1)$$

In the above equations,  $C_D$  is the drag force coefficient,  $S_{hc}$  is the convective Sherwood number taking the value 2 in a quiescent flow, and  $A = 6/(\pi\rho_l)$  is a constant parameter in which  $\rho_l$  is the liquid constant density. The properties of the gas ( $\mu$  viscosity,  $\rho$  density, and  $U_i$  velocity) are obtained at the droplet position from the grid nodes using a third order interpolation algorithm (Guichard *et al.* 1998). These equations have been made dimensionless with  $Re$  as the acoustic Reynolds number of the DNS problem, and  $S_c$  and  $Pr$  are the Schmidt number of the fuel and the Prandtl number, where  $Pr = Sc = 0.7$ .

To construct the thermal budget, we assume all the energy reaching the surface contributes to the droplet skin vaporization without any transfer or accumulation in the liquid core (thin skin approximation, Faeth 1983). With this description, only an infinitely thin layer of fuel around the droplet is heated and vaporized while the temperature and the liquid mass fraction of the droplet core remain constant and equal to the conditions of injection.

The properties of vaporization are characterized by the species Spalding parameter,  $b = Y_F / (Y_F^s - 1)$ , from which the Spalding number is defined:  $B_Y = b^\infty - b^s$ . The fuel mass fractions  $Y_F^s$  and  $Y_F^\infty$  are taken at the surface of the droplet and in the pure gas respectively. Defined in this manner,  $B_Y$  characterizes the diffusion rate of the fuel and may be estimated with three different levels of complexity. In a first approximation  $B_Y$  is assumed constant, then the droplet diameter follows a d-square law,  $\Theta^2(t) = \Theta^2(t=0) - \beta t$ , where  $\beta$  is the vaporization coefficient. Other possibilities are to consider  $B_Y$  as linearly related to the gas temperature around the droplet or to calculate  $B_Y$  as a function of the saturation, the local pressure and temperature, and, eventually, the gaseous fuel mass fraction. The simulations of turbulent mixing have been performed with a constant Spalding number corresponding to situations where the temperature of the spray is close to saturation, whereas the second possibility ( $B_Y = B_Y(T)$ ) is retained for the spray flame calculations.

The flow is described by solving the following equations accounting for the two-way coupling:

$$\begin{aligned} \frac{\partial \rho}{\partial t} + \frac{\partial \rho U_j}{\partial x_j} &= \frac{1}{\mathcal{V}} \sum_k w_v^k \quad , \\ \frac{\partial \rho U_i}{\partial t} + \frac{\partial \rho U_i U_j}{\partial x_j} &= -\frac{\partial P}{\partial x_i} + \frac{1}{R_e} \frac{\partial \sigma_{ij}}{\partial x_j} - \frac{1}{\mathcal{V}} \sum_k (D_i^k - w_v^k V_i^k) \quad , \\ \frac{\partial \rho E_t}{\partial t} + \frac{\partial \rho E_t U_j}{\partial x_j} &= \frac{\partial}{\partial x_i} \left( \frac{\mu C_p}{R_e Pr} \frac{\partial T}{\partial x_i} \right) + \frac{1}{R_e} \frac{\partial \sigma_{ij} U_j}{\partial x_i} - \frac{1}{\mathcal{V}} \sum_k \left[ \frac{1}{2} V_i^k (D_i^k - w_v^k V_i^k) \right] \quad , \\ \frac{\partial \rho Y_F}{\partial t} + \frac{\partial \rho Y_F U_j}{\partial x_j} &= \frac{\partial}{\partial x_i} \left( \frac{\mu}{R_e Sc} \frac{\partial Y_F}{\partial x_i} \right) + \frac{1}{\mathcal{V}} \sum_k w_v^k \quad , \\ \frac{\partial \rho Y_O}{\partial t} + \frac{\partial \rho Y_O U_j}{\partial x_j} &= \frac{\partial}{\partial x_i} \left( \frac{\mu}{R_e Sc} \frac{\partial Y_O}{\partial x_i} \right) \quad , \end{aligned}$$

where  $\mathcal{V}$  is the volume defined in the vicinity of the grid point. In this volume we accumulate the vaporization source from each droplet in order to achieve the coupling between the Eulerian and Lagrangian descriptions.

A third order Runge-Kutta scheme with a minimal data storage method (Wray 1998) is used for time stepping. Spatial derivatives are estimated using the sixth order Lele’s PADE scheme (Lele 1992). Non-reflecting boundary conditions of Poinso and Lele (1992) have been used for calculations with combustion.

### 2.3 DNS parameters

The droplets are organized in clusters (or clouds) homogeneously embedded in a 3D freely decaying turbulence with an initial integral length scale that is twice the mean radius of these clusters (see Fig. 2). The density of droplets in the clusters is chosen to reproduce, in the mean, a near-stoichiometric dilute spray of n-heptane with the stoichiometric value  $Z_{st} = 0.0625$ . Table 1 summarizes the parameters used in the four different simulations with variable Spalding number and, therefore, variable mean vaporization time. To allow comparison of micromixing with and without droplet vaporization, we have also performed a simulation with an infinite value for the Spalding number  $B_Y$  (instantaneously vaporizing droplets).

Case	$B_Y$	$\Theta_0/l_t$	$\tau_t/\tau_V$	$\tau_V/\tau_k$	$Re_{lt}$
$TV_1$	4	0.014	1.37	7.5	104
$TV_2$	2.7	0.014	1.18	8.66	104
$TV_3$	1.9	0.014	0.94	10.97	104
$TV_G$	$\infty$	0.014	$\infty$	0	104

Table 1. Parameters of the simulations ( $65 \times 65 \times 65$ , 10800 droplets organized in 9 clusters): The turbulence is characterized by its integral length scale  $l_t$ , the eddy turnover time  $\tau_t$ , the Kolmogorov time  $\tau_k$ , and the Reynolds number  $Re_{lt} = (u' l_t / \nu) \approx (\tau_t / \tau_k)^2$ . The properties of the spray are:  $\Theta_0$  the initial diameter of the droplets,  $B_Y$  the Spalding number, and its related vaporization time  $\tau_v$ .

### 3. One Droplet Model (ODM)

As mentioned in Section 1, determining both the mean mixture fraction,  $\widetilde{Z}$ , and its fluctuations,  $\widetilde{Z''^2}$ , is a major issue of numerical modeling for nonpremixed turbulent flames (Peters 1986). We will limit our discussion to closure for the RANS/Lagrangian approach where the spray is modeled through a mean lagrangian description (Lixing 1993). The RANS/Lagrangian approach brings an approximation of the mean vaporization rate  $\widetilde{W}_v$  entering the transport equation for  $\widetilde{Z}$ , which is then closed (Lixing 1993). Unfortunately, this method does not close many terms found in the transport equation for  $\widetilde{Z''^2}$ , thus additional modeling is needed.

#### 3.1 Budget equation for $\widetilde{Z''^2}$

The mixture fraction is defined as  $Z = (\Phi Y_F / Y_{F,o} - Y_O / Y_{O,o} + 1) / (\Phi + 1)$ . The mass fractions in pure fuel and pure oxidizer are denoted by  $Y_{F,o}$  and  $Y_{O,o}$ , respectively, and the stoichiometric point is  $Z_{st} = 1 / (1 + \Phi)$ . The equivalence ratio

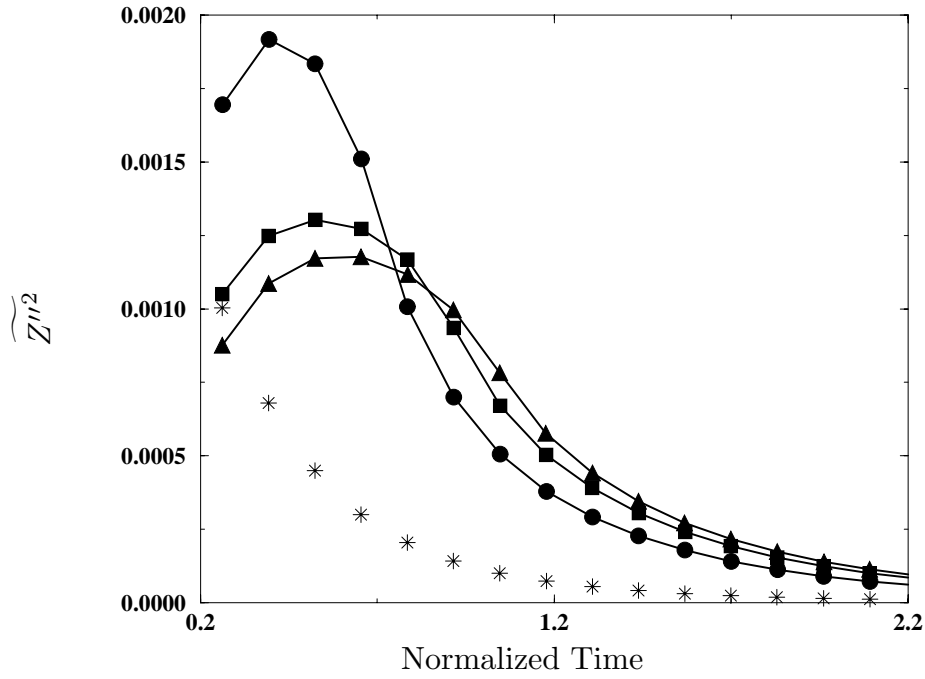


FIGURE 3. Time evolution of the fluctuations  $\widetilde{Z''^2}$ ; the time is normalized by the eddy turn over time. Symbols: \*:  $TV_G$ ; •,  $TV_1$ ; ■,  $TV_2$ ; ▲,  $TV_3$ .

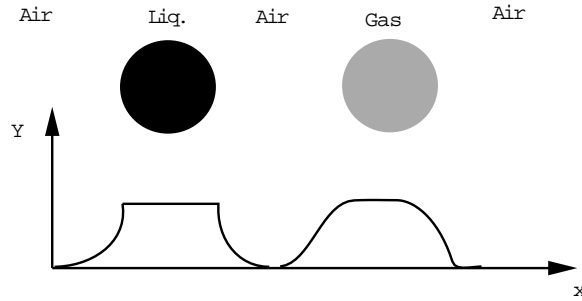


FIGURE 4. Sketch of  $Y_F$  through a drop or a pocket of gas.

of the mixture is  $\Phi = (\nu_O \mathcal{M}_O Y_{F,o}) / (\nu_F \mathcal{M}_F Y_{O,o})$ , with the molecular weights  $\mathcal{M}_O$ ,  $\mathcal{M}_F$  and the stoichiometric coefficients  $\nu_O$ ,  $\nu_F$ ,  $\nu_P$  corresponding to the reaction  $\nu_F Y_F + \nu_O Y_O \rightarrow \nu_P Y_P$ . The transport equation for  $Z$  is:

$$\frac{\partial \rho Z}{\partial t} + \frac{\partial \rho Z U_j}{\partial x_j} = \frac{\partial}{\partial x_i} \left( \rho D \frac{\partial Z}{\partial x_i} \right) + \frac{1}{(1 + \Phi)} \left( \frac{\Phi + Y_{F,o}}{Y_{F,o}} \right) \rho \dot{W}_v,$$

where  $\rho \dot{W}_v = \frac{1}{V} \sum_k \dot{\omega}_k$  is the vaporization rate defined in Section 2.2. From this

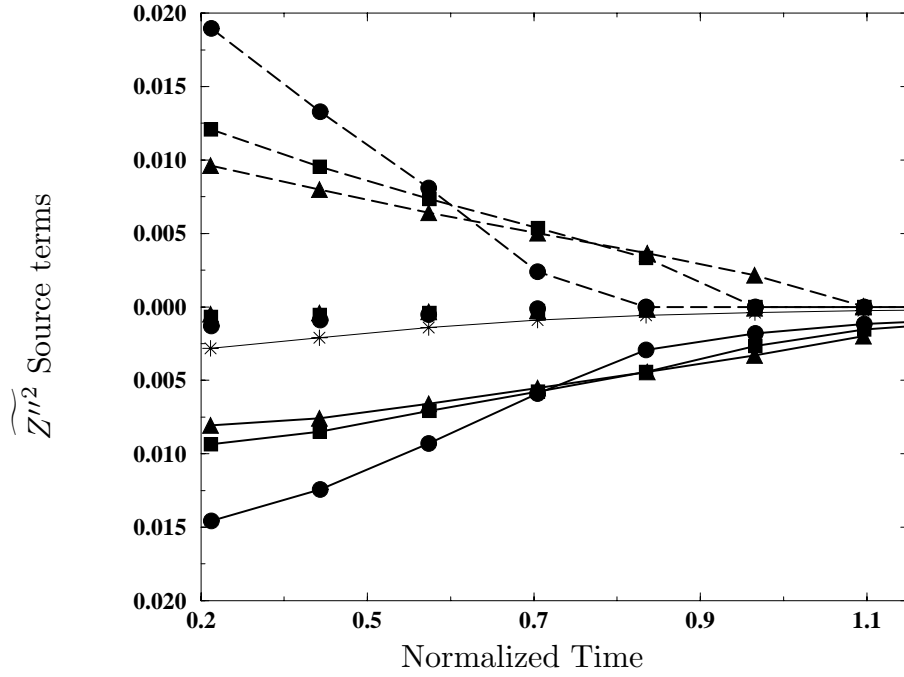


FIGURE 5. Source terms for  $\widetilde{Z}''^2$  (see Eq. (2)). Lines with symbols: Dissipation rate  $\overline{\rho\tilde{\chi}}$ . ---- with symbols:  $\overline{\rho\tilde{S}^+}$ . Symbols:  $\overline{\rho\tilde{S}^-}$ . \*: pure gas mixing simulation  $TV_G$ ; •, ■, and ▲: two-phase simulations  $TV_1$ ,  $TV_2$ ,  $TV_3$  (see table 1).

equation, the balance equation for the fluctuations  $\widetilde{Z}''^2$  may be written,

$$\begin{aligned} \frac{\partial \overline{\rho\tilde{Z}''^2}}{\partial t} + \frac{\partial \overline{\rho\tilde{Z}''^2\tilde{U}_i}}{\partial x_i} = & \underbrace{-\frac{\partial}{\partial x_i} \left( \overline{\rho\tilde{Z}''^2\tilde{U}_i} \right)}_{\text{Turbulent convection}} \underbrace{-2\overline{\rho\tilde{Z}''\tilde{U}_i} \frac{\partial \tilde{Z}}{\partial x_i}}_{\text{Production}} - \underbrace{2\rho D \frac{\partial \tilde{Z}''}{\partial x_i} \frac{\partial \tilde{Z}''}{\partial x_i}}_{\text{Dissipation}} \\ & + \underbrace{2\overline{\rho\tilde{Z}''\dot{W}_v} \left( \frac{1}{(1+\Phi)} \left( \frac{\Phi + Y_{F,o}}{Y_{F,o}} \right) - \tilde{Z} \right)}_{\text{Vaporization}} - \overline{\rho\tilde{Z}''^2\dot{W}_v} \quad , \end{aligned} \quad (2)$$

in which the dissipation rate  $\overline{\rho\tilde{\chi}} = \overline{2\rho D |\nabla \tilde{Z}''|^2}$  appears with two unclosed source terms that are directly related to spray vaporization. The objective is to model those two terms:

$$\overline{\rho\tilde{S}^+} = 2\overline{\rho\tilde{Z}''\dot{W}_v} \left( \frac{1}{(1+\Phi)} \left( \frac{\Phi + Y_{F,o}}{Y_{F,o}} \right) - \tilde{Z} \right) \quad \text{and} \quad \overline{\rho\tilde{S}^-} = -\overline{\rho\tilde{Z}''^2\dot{W}_v} \quad .$$

The time evolution of  $\widetilde{Z}''^2$  is considered first. Since the distributions of fuel and oxidizer are homogeneous, the equation for  $\widetilde{Z}''^2$  reduces to  $\partial(\overline{\rho\tilde{Z}''^2})/\partial t = \overline{\rho\tilde{S}^+} + \overline{\rho\tilde{S}^-} - \overline{\rho\tilde{\chi}}$ . Furthermore, in the case of pure gas mixing obtained for an infinitely small vaporization time ( $TV_\infty$  in table 1),  $\widetilde{Z}''^2$  can be expressed as  $\partial(\overline{\rho\tilde{Z}''^2})/\partial t =$

$-\overline{\rho\chi}$ . As expected (Dopazo 1994), one observes in Fig. 3 the well-known exponential decay of  $\widetilde{Z''^2}$  for this reference situation.

When the liquid phase is present,  $\widetilde{Z''^2}$  behaves differently. Fluctuations of mixture fraction are generated by the local sources of fuel, and  $\widetilde{Z''^2}$  increases quickly to reach a maximum point. The value of  $\widetilde{Z''^2}$  at this maximum depends on the characteristic time of vaporization (Fig. 3), when the shorter the vaporization time, the larger this value. After reaching this maximum, turbulent micro-mixing becomes the dominant effect and the exponential decay is recovered.

A previous study had discussed how the mean turbulent mixing time and related quantities are dramatically affected by the liquid phase (Réveillon *et al.* 1998). In dilute spray, this is partly due to the impact of vaporization source on the small scales of the fuel field. Because of the non-diffusing reservoir of fuel in the core of the drop, the value taken by  $|\nabla Y_F|$  when  $Y_F \rightarrow 1$  tends to be larger in the case of droplets than for a pocket of gas (Fig. 4). One consequence of this is the increase in dissipation rate  $\overline{\rho\chi}$  following the introduction of the spray (Fig. 3).

It is also observed in Fig. 5 that the production term  $\overline{\rho S^+}$  is positive and of the same order as the dissipation rate,  $\overline{\rho\chi}$ , while  $\overline{\rho S^-}$  is small. This is expected since vaporization first generates large positive value of  $Z''$ , and  $\overline{\rho S^+}$  is linear in  $Z''$ , whereas  $\overline{\rho S^-}$  is quadratic in  $Z''$ .

### 3. ODM closure for $\overline{\rho S^+}$ and $\overline{\rho S^-}$

The unknowns contained in the terms  $\overline{\rho S^+}$  and  $\overline{\rho S^-}$  are  $\overline{\rho Z'' \dot{W}_v}$  and  $\overline{\rho Z''^2 \dot{W}_v}$ . Introducing  $\tilde{P}(Z^*)$ , the probability density function (pdf) of  $Z$ , we will reduce the modeling of  $\overline{\rho S^+}$  and  $\overline{\rho S^-}$  to the determination of  $\left(\overline{\dot{W}_v} \mid Z^*\right)$ , the mean of the vaporization rate calculated for a particular value  $Z = Z^*$  of the mixture fraction. It turns out that this conditional mean can be approximated from the exact solution of a dilute spray problem in a quiescent flow. In calculations of practical combustion chambers, a beta function (Bray 1996) is usually utilized for presuming  $\tilde{P}(Z^*)$  from  $\tilde{Z}$  and  $\tilde{Z''^2}$ . One may write,

$$\overline{\rho Z'' \dot{W}_v} = \bar{\rho} \int_0^1 (Z - \tilde{Z}) \left(\overline{\dot{W}_v} \mid Z^*\right) \tilde{P}(Z^*) dZ^*$$

and

$$\overline{\rho Z''^2 \dot{W}_v} = \bar{\rho} \int_0^1 (Z - \tilde{Z})^2 \left(\overline{\dot{W}_v} \mid Z^*\right) \tilde{P}(Z^*) dZ^*$$

In the above equations,  $\left(\overline{\dot{W}_v} \mid Z^*\right) = \left(\overline{\frac{1}{V} \sum_n \dot{\omega}_v^k} \mid Z = Z^*\right)$  depends on the statistics of both the diameters  $\Theta$  of the droplets and the Spalding number  $B_Y$ , so we consider the case of a constant  $B_Y$  first.

In the class of two phase flow problems described with dilute spray, the droplets are smaller than the Kolmogorov scale and tend to follow the turbulent structures



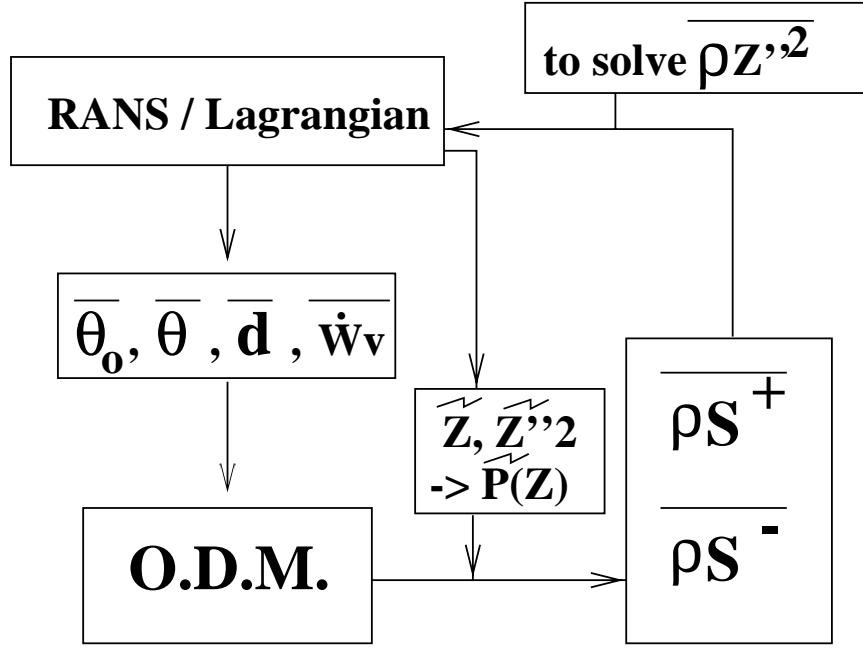


FIGURE 6. Sketch of the ODM procedure.

(weak drag force). As a consequence, during vaporization large values of  $Z$  are expected in zones where high vaporization rates exist. Moreover, one should observe the largest values of  $\left(\overline{\dot{W}_v} \mid Z^*\right)$  in the vicinity of  $Z^* = Z_{max}$ , the maximum value taken by the mixture fraction in the flow at a particular time. Hence, we anticipate  $\left(\overline{\dot{W}_v} \mid Z^*\right)$  as being a monotonic function of  $Z^*$ ,

$$\left(\overline{\dot{W}_v} \mid Z^*\right) = \left(\alpha_{B_Y}(\overline{\Theta}, \overline{d}) Z^*\right)^n, \quad (3)$$

where  $\overline{\Theta}$  and  $\overline{d}$  are the mean diameter of the droplets and the mean spray density provided by the RANS/Lagrangian solver, and  $n$  is a parameter dynamically determined and accounting for the effect of turbulence on the spray. The physical properties of the liquid phase enter ODM through the function  $\alpha_{B_Y}(\overline{\Theta}, \overline{d})$ . Considering the spray to be homogeneous, we estimate  $\alpha_{B_Y}(\overline{\Theta}, \overline{d})$  by replacing the collection of droplets by a unique drop of initial diameter  $\overline{\Theta}_0$ , vaporizing in a quiescent flow of volume  $1/\overline{d}$  where  $\overline{d}$  is the mean spray density. From Eq. (1) giving the vaporization

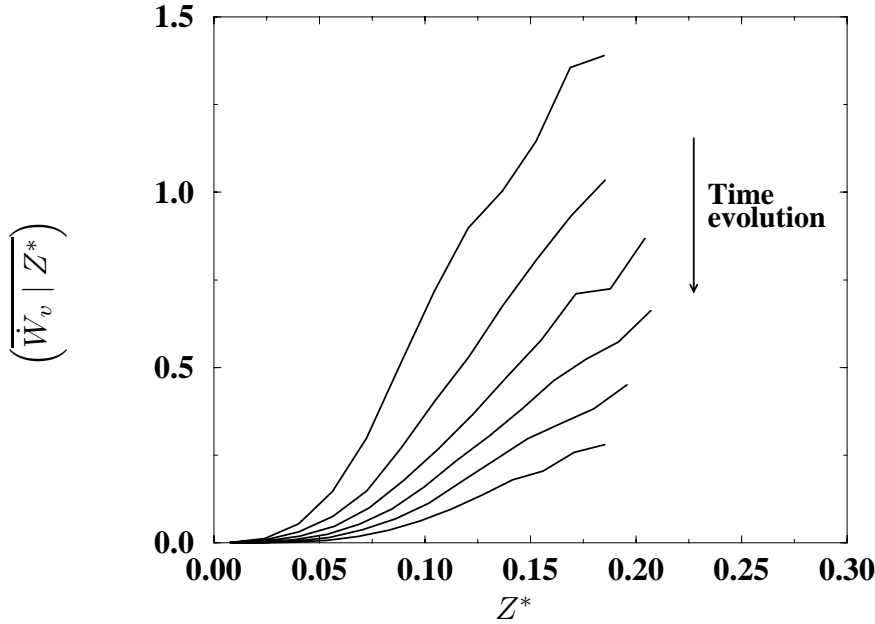


FIGURE 7. Time evolution of  $\left(\overline{\dot{W}_v | Z^*}\right)$ , the conditional mean value of the vaporization rate.

rate, we write for this unique drop:

$$\rho \dot{W}_v(\bar{\Theta}, \bar{d}) = \pi \frac{\mu S_{hc}}{ReSc} \ln(1 + B_Y) \bar{\Theta} \bar{d} \quad ,$$

$$\rho Z^*(\bar{\Theta}, \bar{d}) = \frac{1}{(1 + \Phi)} \left( \frac{\Phi + Y_{F,o}}{Y_{F,o}} \right) \rho_l \left( \bar{\Theta}_o^3 - \bar{\Theta}^3 \right) \bar{d} \quad .$$

One may then calculate  $\alpha_{B_Y}(\bar{\Theta}, \bar{d})$  by combining the behavior of the isolated droplet with the proposed closure for the conditional source (Eq. (3)),

$$\dot{W}_v(\bar{\Theta}, \bar{d}) = \left( \alpha_{B_Y}(\bar{\Theta}, \bar{d}) Z^*(\bar{\Theta}) \right)^n \quad .$$

leading to:

$$\alpha_{B_Y}(\bar{\Theta}, \bar{d}) = \frac{\left( \pi \frac{\mu S_{hc}}{\rho ReSc} \ln(1 + B_Y) \bar{\Theta} \bar{d} \right)^{1/n}}{\left( \frac{1}{(1 + \Phi)} \left( \frac{\Phi + Y_{F,o}}{Y_{F,o}} \right) \rho_l \left( \bar{\Theta}_o^3 - \bar{\Theta}^3 \right) \bar{d} \right)} \quad .$$

When using ODM,  $\bar{\Theta}_0$  is the initial mean diameter of the droplets, for instance, their mean diameter at the exit of an injection system.

The coupling between ODM and a CFD code is sketched in Fig. 6. Part of this coupling is achieved via the mean vaporization rate  $\widetilde{\dot{W}_v}$ . This rate is provided by the RANS/Lagrangian solver, and the ODM approximation of  $\left(\overline{\dot{W}_v | Z^*}\right)$  must capture  $\widetilde{\dot{W}_v}$ , resulting in the constraint:

$$\widetilde{\dot{W}_v} = \int_0^1 \left( \overline{\dot{W}_v | Z^*} \right) \tilde{P}(Z^*) dZ^* = \int_0^1 \left( \alpha_{B_Y}(\bar{\Theta}) Z^* \right)^n \tilde{P}(Z^*) dZ^* \quad , \quad (4)$$

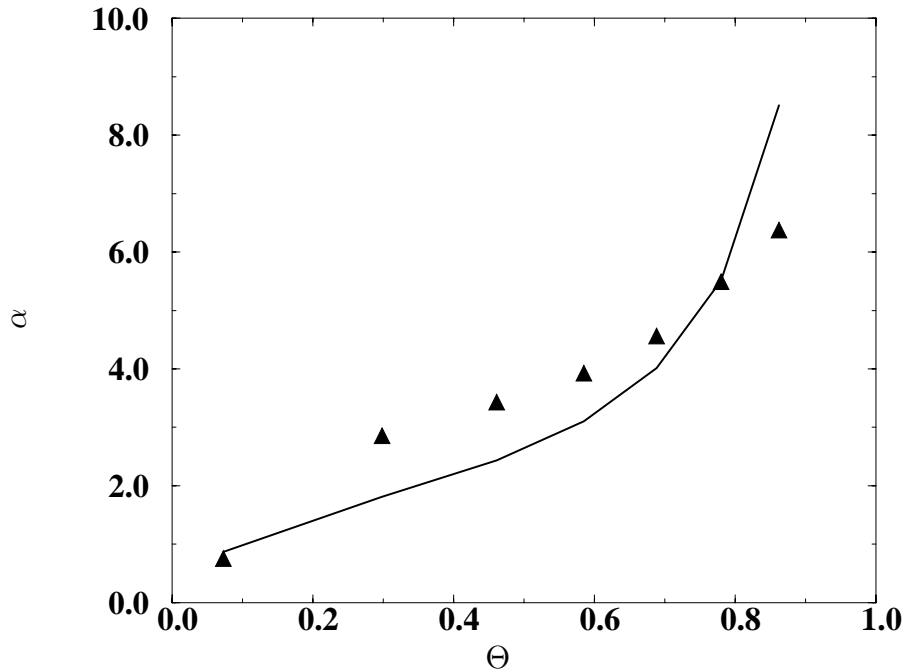


FIGURE 8. Comparison of the value of  $\alpha$  given by ODM (—) and by DNS ( $\blacktriangle$ ).

Equation 4 is then utilized to determine the parameter  $n$ . Here the DNS is used to extract  $\widetilde{W}_v$ , and  $n$  takes on values between 1.8 and 2.2. In practical problems, we expect  $n$  to depend on the turbulent spray regime. From the DNS,  $(\overline{\widetilde{W}_v} | Z^*)$  features a parabolic shape which depends on time (Fig. 7). In Fig. 8 an interesting agreement is observed when the function  $\alpha_{B_Y}(\overline{\Theta}, \overline{d})$  is measured from DNS and compared with the estimation given by ODM (Eq. 4).

We have computed with ODM the two terms  $\overline{\rho S^+}$  and  $\overline{\rho S^-}$ , and the comparison with DNS presented in Fig. 9 is satisfactory. Even though this does not appear as a major shortcoming so far, notice that the fluctuations of  $\widetilde{W}_v$  for a given value of  $Z$  are not directly introduced in this closure.

#### 4. A challenging problem for DNS

We now discuss some preliminary results which represent a first step towards a full DNS of turbulent spray combustion. Droplets of fuel have been injected in a two-dimensional double-wake configuration, and a flame is stabilized on the liquid jet while simple step chemistry is retained. The Spalding number  $B_Y$  depends on temperature; therefore, the stabilization of the flame results from the diffusion of heat vaporizing the liquid. A diffusion flame develops, and its main body is attached to the spray by a triple flame (Ruetsch *et al.* 1995) composed of a rich premixed flame where the droplets are vaporizing and two lean premixed flames on both sides of the jet (Fig. 10). The vorticity field shows that heat release affects the flow through gas expansion even at the end of the core of the dilute spray. Those simulations suggest that, despite the large number of physical parameters

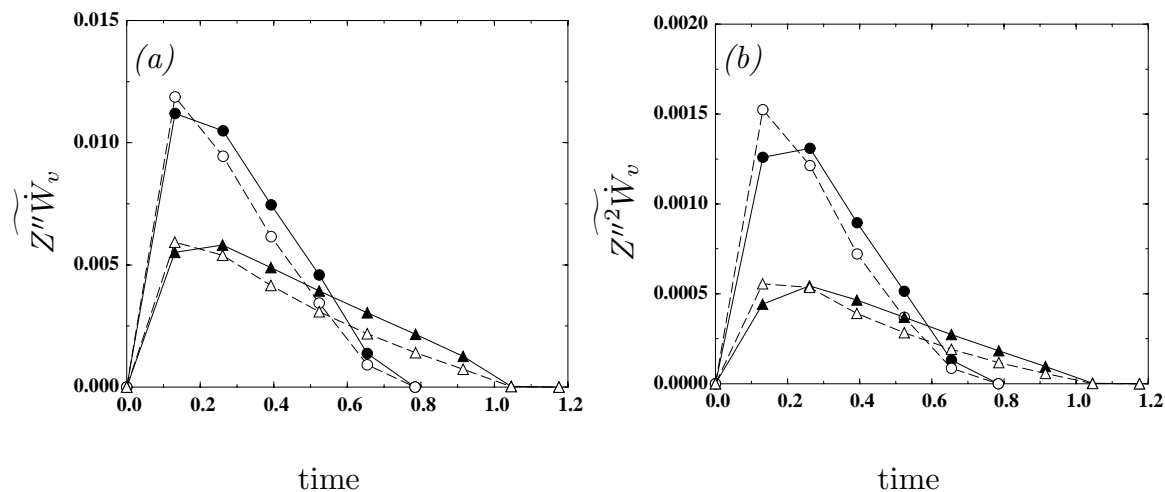


FIGURE 9. Comparisons DNS / ODM. (a)  $\widetilde{S^+}$ , (b)  $\widetilde{S^-}$ . Symbols: • : DNS-TV1; ○ : ODM-TV1; ▲ : DNS-TV3; △ : ODM-TV3.

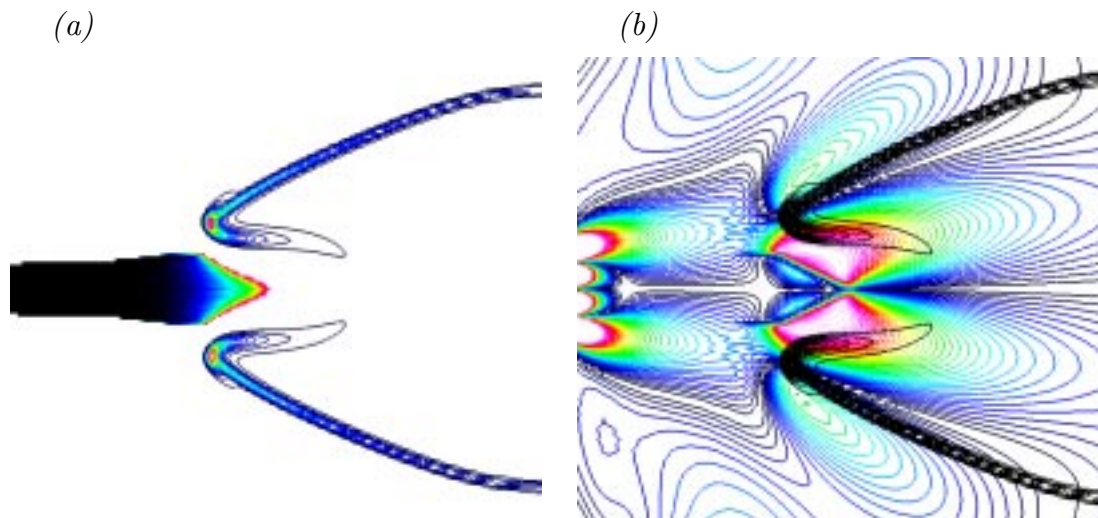


FIGURE 10. Flame attached on a spray. (a) Reaction rate around vaporizing droplets. (b) Reaction rate and vorticity.

embedded in liquid fuel combustion, DNS will soon emerge as an efficient tool to help understand and model turbulent spray combustion.

## 5. Conclusion

Direct numerical simulations of turbulent mixing of a vaporizing spray have been performed. From the results, closures are proposed for the source terms appearing in the transport equation for the fluctuations of the mixture fraction. They are based on a simple One Droplet Model utilized to express the conditional mean of the turbulent vaporization rate. In the same context, first DNS of a flame attached

to liquid jet have been performed.

### Acknowledgment

This work has benefited from many stimulating and exciting discussions with the members of the CTR Summer Program; in particular, the authors gratefully acknowledge their CTR hosts Prof. J. Ferziger, and Drs. G. Ruetsch and J. Oefelein.

### REFERENCES

- BORGHI R. 1988 Turbulent combustion modeling. *Prog. Energy Combust. Sci.* **14**, 245-292.
- BORGHI, R. 1996 Background on droplets and spray. *Combustion and Turbulence in Two-Phase Flows. von Karman Institute for Fluid Dynamics, Lecture Series 1996-02, (Eds M. Manna & D. Vandromme) VKI-Belgium.*
- BRAY, K. N. C. 1996 The Challenge of turbulent combustion. *Proceedings of the 26th Symp. (Int.) on Combustion, Naples.* The Combustion Institute, Pittsburgh.
- CHIU H. H. & KIM H. Y. & CROKE E. J. 1982 Internal group combustion of liquid droplets. *Proceedings of the nineteenth Symposium (International) on combustion.* **19**, 971-980.
- DOPAZO, C. 1994 Recent developments in pdf methods. In *Turbulent Reacting Flows.* Academic Press London (Eds P. A. Libby and F. A. Williams), 375-474.
- ELGOBASHI S. & TRUESDELL G. C. 1992 Direct numerical simulation of particle dispersion in a decaying isotropic turbulence. *J. Fluid Mech.* **242**, 655-700.
- FAETH G. M. 1983 Evaporation and combustion of sprays. *Prog. Energy Combust. Sci.* **9**, 1-76.
- GUICHARD L. & LECORDIER B. & RÉVEILLON J. 1998 Evaluation des algorithmes utilisés en PIV grâce à la simulation numérique directe. *6ieme Congrès francophone de Vélocimétrie Laser.* **F-5**, Saint-Louis, France.
- GUICHARD L. & VERVISCH L. & DOMINGO P. 1995 Two-dimensional weak shock-vortex interaction in a mixing zone. *AIAA J.* **33**, 1797-1802.
- KUO K. K. 1986 *Principles of combustion.* John Wiley and Sons.
- LAW C. K. Recent advances in droplet vaporization and combustion 1982. *Prog. Energy Combust. Sci.* **8**, 171-201.
- LELE S. K. 1992 Compact finite difference schemes with spectral like resolution. *J. Comput. Phys.* **103**, 16-42.
- LIÑÁN, A. 1974 The asymptotic structure of counterflow diffusion flames for large activation energies. *Acta Astronautica.* **1**, 1007.
- LIXING, Z. 1993 *Theory and numerical modeling of turbulent gas-particle flows and combustion.* Science Press and CRC Press, Inc. ISBN 0-8493-7721-8.

- PETERS, N. 1986 Laminar flamelet concepts in turbulent combustion. In *Proceedings of the 21st Symposium (international) on Combustion, Irvine*. The Combustion Institute Pittsburgh, 1231-1250.
- PIERCE, C. D. & MOIN, P. 1998 Large eddy simulation of a confined coaxial jet with swirl and heat release. *AIAA 98-2892*, 29th AIAA Fluid Dynamics Conference, Albuquerque, NM June 15-18.
- POINSOT, T., CANDEL, S. & TROUVÉ, A. 1996 Direct numerical simulation of premixed turbulent combustion. *Prog. Energy Combust. Sci.* **12**, 531-576.
- POINSOT T. & LELE S. K. 1992 Boundary conditions for direct simulations of compressible viscous flows. *J. Comput. Phys.* **101**, 104-129.
- RÉVEILLON J. & BRAY K. N. C. & VERVISCH L. 1998 DNS study of spray vaporization and turbulent micro-mixing. *AIAA 98-1028*.
- RUETSCH, G. R., VERVISCH, L. & LIÑÁN, A. 1995 Effects of heat release on triple flame. *Phys. Fluids.* **7**, (6) 1447-1454.
- SIRIGNANO W. A. 1983 Fuel droplet vaporization and spray combustion theory. *Prog. Energy Combust. Sci.* **9**, 291-322.
- VERVISCH L. & POINSOT T. 1998 Direct numerical simulation of non-premixed turbulent flame. *Ann. Rev. Fluid Mech.* **30**, 655-692.
- WRAY A. A. 1998 Minimal storage time-advancement schemes for spectral methods. Personal communication.